

Density fluctuation in baryon-rich quark matter

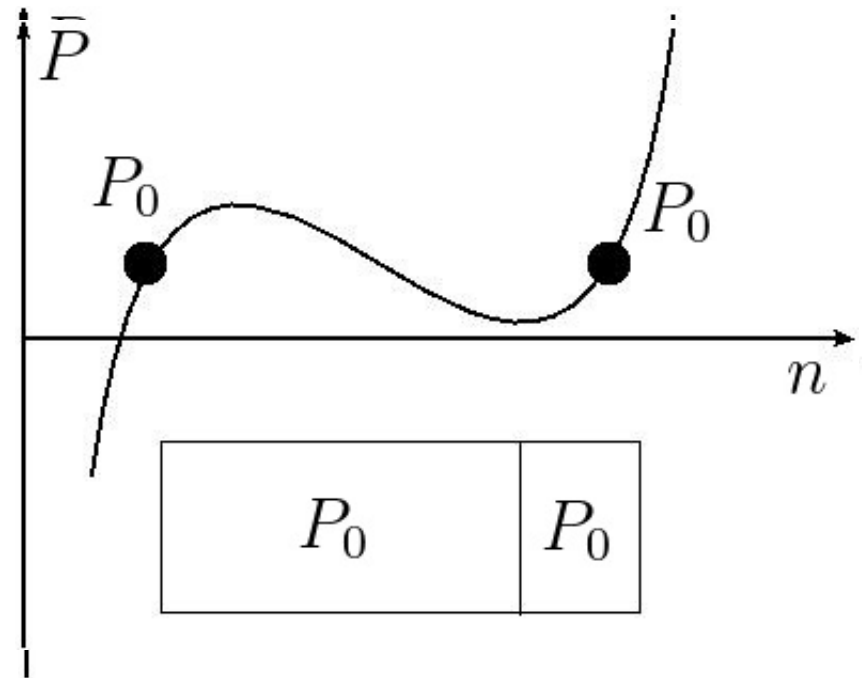
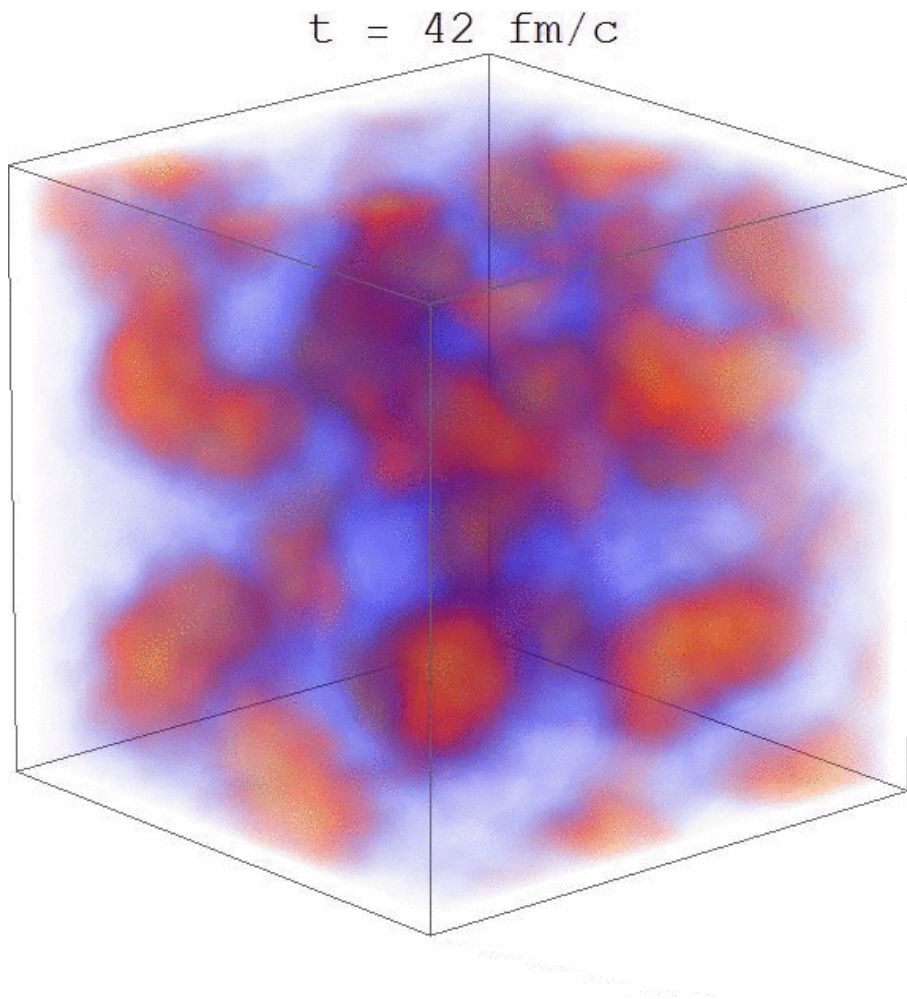
Che-Ming Ko
Texas A&M University

- ☐ Introduction: Spinodal instability
- ☐ The NJL and PNJL models
- ☐ Linear response theory for unstable modes
- ☐ Quark matter in a box
- ☐ Expanding quark matter
- ☐ Summary

Based on work with Feng Li [PRC 93, 035215 (2016); 95, 055203 (2017)]



Spinodal Instability



$$\left(\frac{\partial P}{\partial n}\right)_T < 0 \quad \text{or} \quad \left(\frac{\partial P}{\partial n}\right)_S < 0$$

- Such as the gas-liquid transition in nuclear matter and the quark to hadronic matter transition at finite baryon chemical potential.

Polyakov Nambu-Jona-Lasinio (PNJL) model

$$\begin{aligned}\mathcal{S}_{\text{PNJL}}[q, \bar{q}, \phi] = & \beta V \mathcal{U}(\Phi, \bar{\Phi}, T) - \int_0^\beta d^4x \left\{ \bar{q}(-\gamma^0(\partial_\tau + i\bar{\phi}) \right. \\ & + i\boldsymbol{\gamma} \cdot \boldsymbol{\nabla} - m_0)q + \frac{G_S}{2} \sum_{a=0}^8 \left[(\bar{q}\lambda^a q)^2 + (\bar{q}i\gamma_5\lambda^a q)^2 \right] \\ & \left. - G_V(\bar{q}\gamma_\mu q)^2 - K \left[\det_f \left(\bar{q}(1 + \gamma_5)q \right) + \det_f \left(\bar{q}(1 - \gamma_5)q \right) \right] \right\}\end{aligned}$$

- Quarks interact via contact interactions.
- The scalar interaction is attractive, while the vector interaction is repulsive.
- G_S and K are determined by fitting the pion and kaon masses and their decay constants, while G_V is a parameter.
- Φ is the Polyakov loop, which is a measure of $e^{-\beta F}$ with F being the free energy due to a colour source,

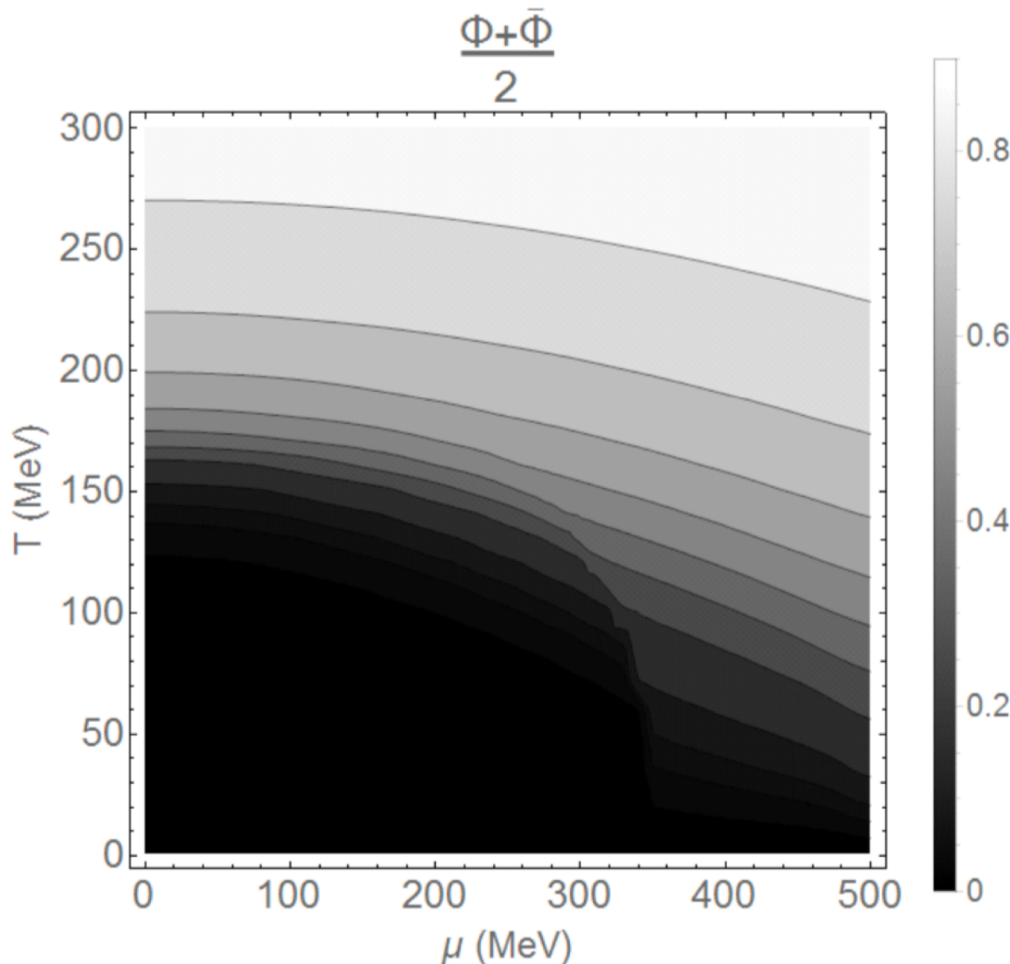
$$\Phi \equiv \frac{1}{N_c} \text{Tr} \left[\mathcal{P} \exp \left(i \int_0^\beta d\tau \phi \right) \right] = \frac{1}{3} \text{Tr} e^{i\phi/T} = \begin{cases} 0 & T < T_0 \\ 1 & T \rightarrow \infty \end{cases}$$

where ϕ is the gauge field, and is the order parameter for confinement-deconfinement transition and is fitted to lattice gauge calculations.

$$\frac{\mathcal{U}(\Phi, \bar{\Phi}, T)}{T^4} = -\frac{1}{2}a(T)\bar{\Phi}\Phi + b(T) \ln[1 - 6\bar{\Phi}\Phi + 4(\bar{\Phi}^3 + \Phi^3) - 3(\bar{\Phi}\Phi)^2]$$

$$a(T) = a_0 + a_1 \left(\frac{T_0}{T}\right) + a_2 \left(\frac{T_0}{T}\right)^2, \quad b(T) = b_3 \left(\frac{T_0}{T}\right)^3$$

Fitting lattice results $\rightarrow a_0 = 3.51, a_1 = -2.47, a_2 = 15.2, b_3 = -1.75$



With $T_0 = 210$ MeV \rightarrow
 171 MeV for deconfinement
 transition and 203 MeV for
 chiral phase transition at zero
 baryon chemical potential

Mean-field approximation

In the mean-field approximation, the action becomes bilinear in quark fields

$$\mathcal{S}_{\text{PNJL}}[q, \bar{q}, \phi] \approx \beta V \mathcal{U}(\Phi, \bar{\Phi}, T) - \int_0^\beta d^4x \left\{ \sum_{i,j,k;\text{cyclic}} \bar{q}_i \left(-\gamma^0(\partial_\tau + i\bar{\phi} - \mu - i\mathbf{u} \cdot \nabla) + i\boldsymbol{\gamma} \cdot \nabla - m_{0i} + 2G_S \sigma_i - 2G_S \gamma_5 \theta_i - 2K(\sigma_j \sigma_k + \theta_j \theta_k) - 2K \gamma_5(\sigma_j \theta_k + \theta_j \sigma_k) - 2G_V \gamma^\mu j_\mu \right) q_i + \sum_i G_S(\sigma_i^2 - \theta_i^2) - 2K \prod_i (\sigma_i + \theta_i) - 2K \prod_i (\sigma_i - \theta_i) - G_V j^2 \right\}$$

where $\sigma_i \equiv \langle \bar{q}_i q_i \rangle$, $\theta_i \equiv \langle \bar{q}_i \gamma_5 q_i \rangle$, $j_\mu \equiv \langle \sum_i \bar{q}_i \gamma_\mu q_i \rangle$

Quarks thus acquire the effective masses

$$M_i = m_{0i} - 2G_S \sigma_i + 2K(\sigma_j \sigma_k + \theta_j \theta_k)$$

with $\theta_i = 0$

$$\sigma_i = 6 \int_0^\Lambda \frac{d^3 \mathbf{p}}{(2\pi)^3} \frac{M_i}{E_{\mathbf{p}_i}} (f_0(\xi_i; \Phi, \bar{\Phi}) + f_0(\xi'_i; \bar{\Phi}, \Phi) - 1)$$

where
$$f_0(\xi_i; \Phi, \bar{\Phi}) = \frac{\bar{\Phi}\xi_i^2 + 2\Phi\xi_i + 1}{\xi_i^3 + 3\bar{\Phi}\xi_i^2 + 3\Phi\xi_i + 1}$$

with
$$\xi_i = \exp(\beta(E_{p_i} - \mu + \mathbf{u} \cdot \mathbf{p} + 2G_V j^0)) \quad \xi'_i = \exp(\beta(E_{p_i} + \mu - \mathbf{u} \cdot \mathbf{p} - 2G_V j^0))$$

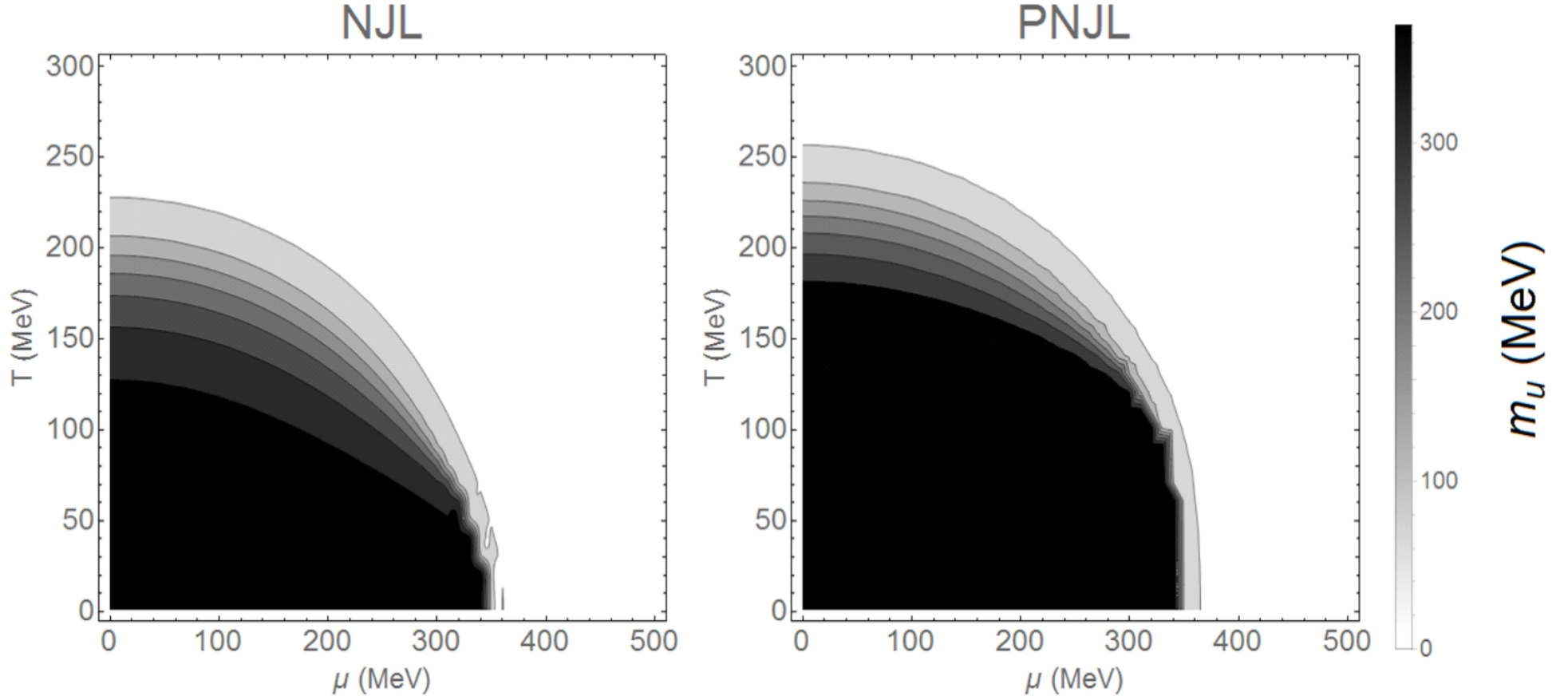


Figure 2.2: Effective u and d quark masses as functions of T and μ calculated from the NJL model (left window) and the PNJL model (right window) with model parameters $\Lambda = 0.6023$ GeV, $G_S = 3.67\Lambda^2$, and $K = 12.36\Lambda^5$.

Strange quark mass in quark matter

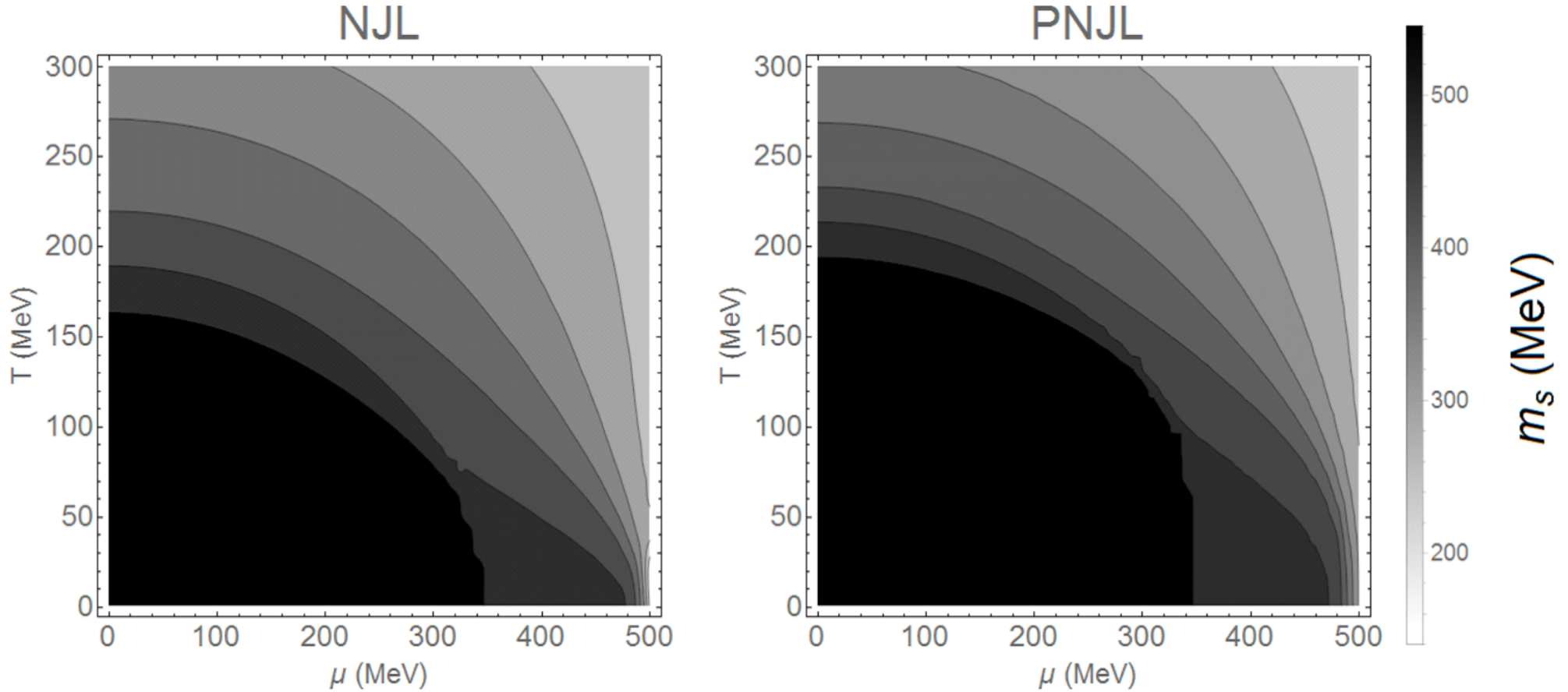
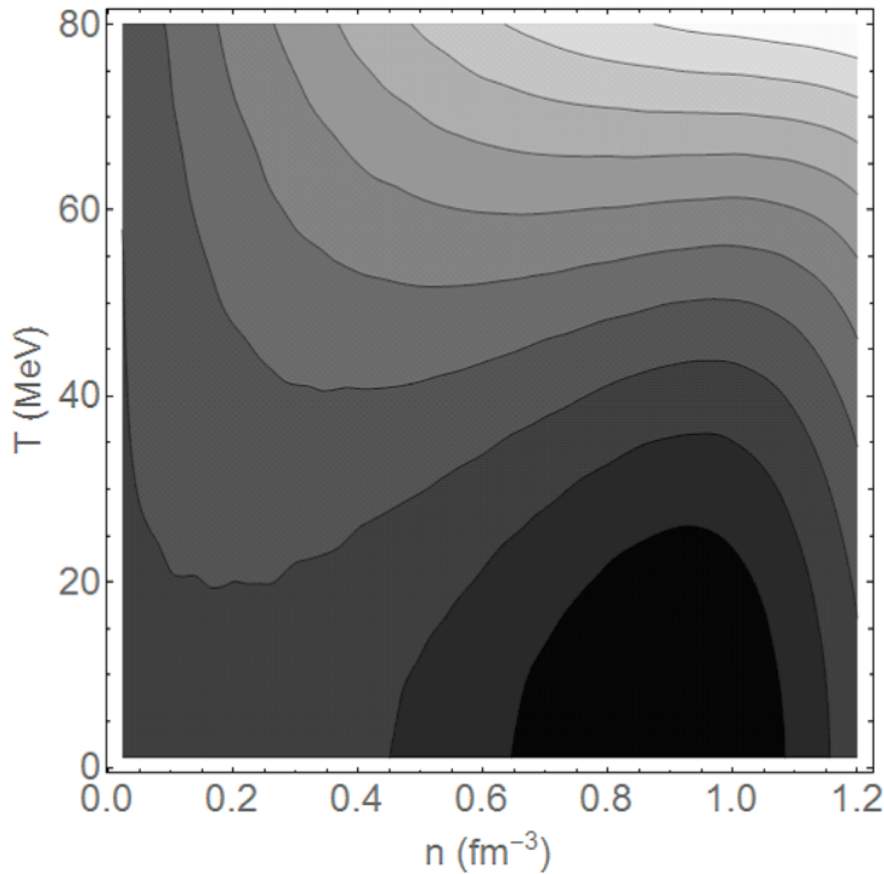


Figure 2.3: Effective s quark mass as a function of T and μ calculated from the NJL model (left window) and the PNJL model (right window) with model parameters $\Lambda = 0.6023$ GeV, $G_S = 3.67\Lambda^2$, and $K = 12.36\Lambda^5$.

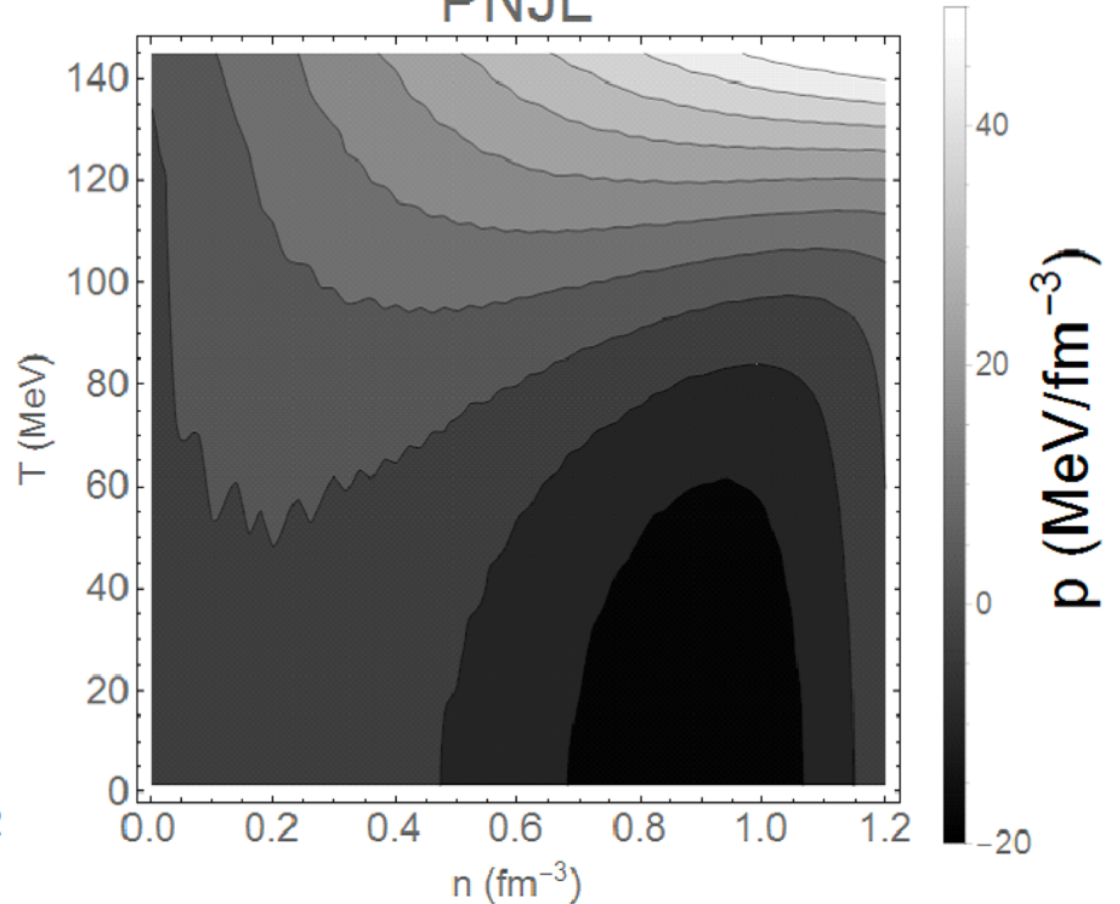
Pressure of quark matter can be calculated from the grand partition function or potential

$$-PV = \Omega(T, \mu) \equiv -(\beta V)^{-1} \ln \left[\int d\bar{q} dq d\Phi d\bar{\Phi} e^{-\int_0^\beta d\tau \int d^3x \mathcal{S}_{\text{PNJL}}(q, \bar{q}, \phi)} \right]$$

NJL

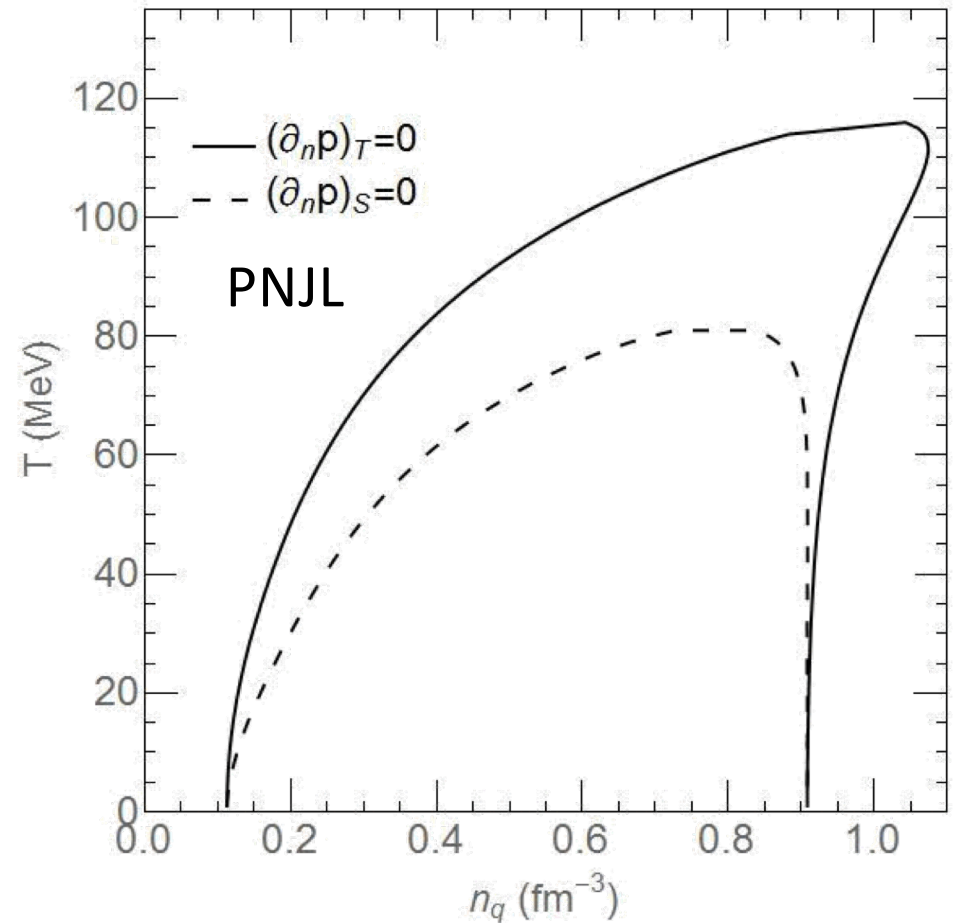
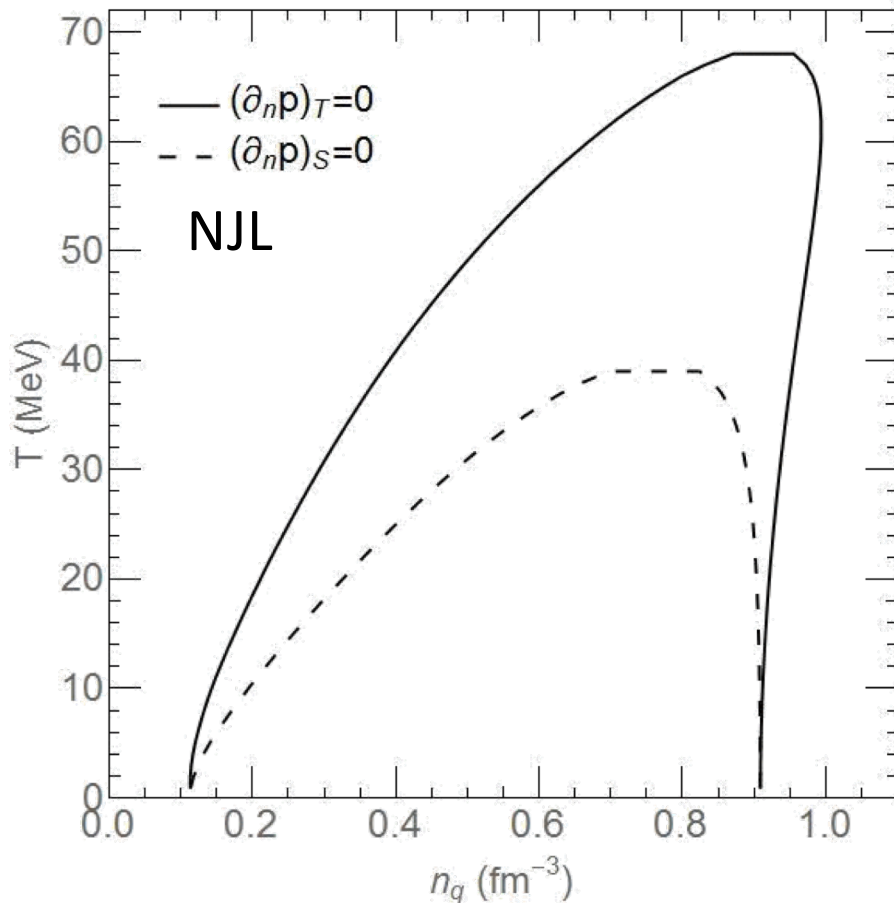


PNJL



Spinodal instability in NJL and PNJL models

Thermodynamic consideration



- Region of spinodal instability is larger in PNJL than in NJL.

Linear response theory

Time evolution of the expectation value of a physical observable A

$$\langle A(t) \rangle = \text{tr}[\rho(t)A_S] \quad \rho(t) = \mathcal{U}(t, t_0)\rho(t_0)\mathcal{U}^\dagger(t, t_0)$$

where the time evolution operator

$$\mathcal{U}(t, t_0) = e^{-i(H_0 + H')(t - t_0)}$$

Linearize the time evolution operator

$$\mathcal{U}(t, t_0) \approx \mathcal{U}_0(t, t_0) - i \int_{t_0}^t dt' \mathcal{U}_0(t, t') H'(t') \mathcal{U}_0(t', t_0)$$

→ linearized density matrix

$$\rho(t) \approx \rho_0(t) - i \int_{t_0}^t dt' \mathcal{U}_0(t, t_0) [H'_I(t'), \rho(t_0)] \mathcal{U}_0^\dagger(t, t_0)$$

and

$$\delta \langle A(t) \rangle \approx i \int d\bar{t} \theta(t - \bar{t}) \langle [H'_I(\bar{t}), A_I(t)] \rangle_0$$

For perturbations proportional to density fluctuations

$$H'_I = \sum_{i=1}^3 \int d^3\mathbf{x} [\bar{q}_i q_i \delta M_i + 2G_V \delta j_\mu (\bar{q}_i \gamma^\mu q_i)]$$

where

$$\delta M_i = -2G_S \delta \langle \bar{q}q \rangle_i - 2K \sum_{j,k=1; i \neq j \neq k}^3 \langle \bar{q}q \rangle_j \delta \langle \bar{q}q \rangle_k$$

$$\delta \langle \bar{q}q(x) \rangle_i \approx i \sum_{j=1}^3 \int d^4\bar{x} \theta(t - \bar{t}) \left\{ \langle [\bar{q}_j(\bar{x}) q_j(\bar{x}), \bar{q}_i(x) q_i(x)] \rangle_0 \delta M_j(\bar{x}) \right. \\ \left. + 2G_V \langle [\bar{q}_j(\bar{x}) \gamma^\nu q_j(\bar{x}), \bar{q}_i(x) q_i(x)] \rangle_0 \delta j_\nu(\bar{x}) \right\}$$

$$\delta \langle j^\mu(x) \rangle \approx i \sum_{i,j=1}^3 \int d^4\bar{x} \theta(t - \bar{t}) \left\{ \langle [\bar{q}_j(\bar{x}) q_j(\bar{x}), \bar{q}_i(x) \gamma^\mu q_i(x)] \rangle_0 \delta M_j(\bar{x}) \right. \\ \left. + 2G_V \langle [\bar{q}_j(\bar{x}) \gamma^\nu q_j(\bar{x}), \bar{q}_i(x) \gamma^\mu q_i(x)] \rangle_0 \delta j_\nu(\bar{x}) \right\}$$

Homogeneous linear algebraic equations for density fluctuations

$$0 = \int d\bar{x} \begin{pmatrix} \delta(x-\bar{x}) - \chi_{11}(x-\bar{x}) & -\chi_{12}(x-\bar{x}) & \cdots \\ -\chi_{21}(x-\bar{x}) & \ddots & \vdots \\ \vdots & \cdots & \ddots \end{pmatrix} \begin{pmatrix} \delta\sigma_q(\bar{x}) \\ \delta\sigma_s(\bar{x}) \\ \delta j^\mu(\bar{x}) \end{pmatrix}$$

where

$$\begin{aligned} \chi_{\sigma\sigma}(x) &\equiv \theta(t) \langle [\bar{q}(x)q(x), \bar{q}(0)q(0)] \rangle_0 \\ \chi_{\sigma j}^\mu(x) &\equiv \theta(t) \langle [\bar{q}(x)\gamma^\mu q(x), \bar{q}(0)q(0)] \rangle_0 \\ \chi_{jj}^{\mu\nu}(x) &\equiv \theta(t) \langle [\bar{q}(x)\gamma^\mu q(x), \bar{q}(0)\gamma^\nu q(0)] \rangle_0 \end{aligned}$$

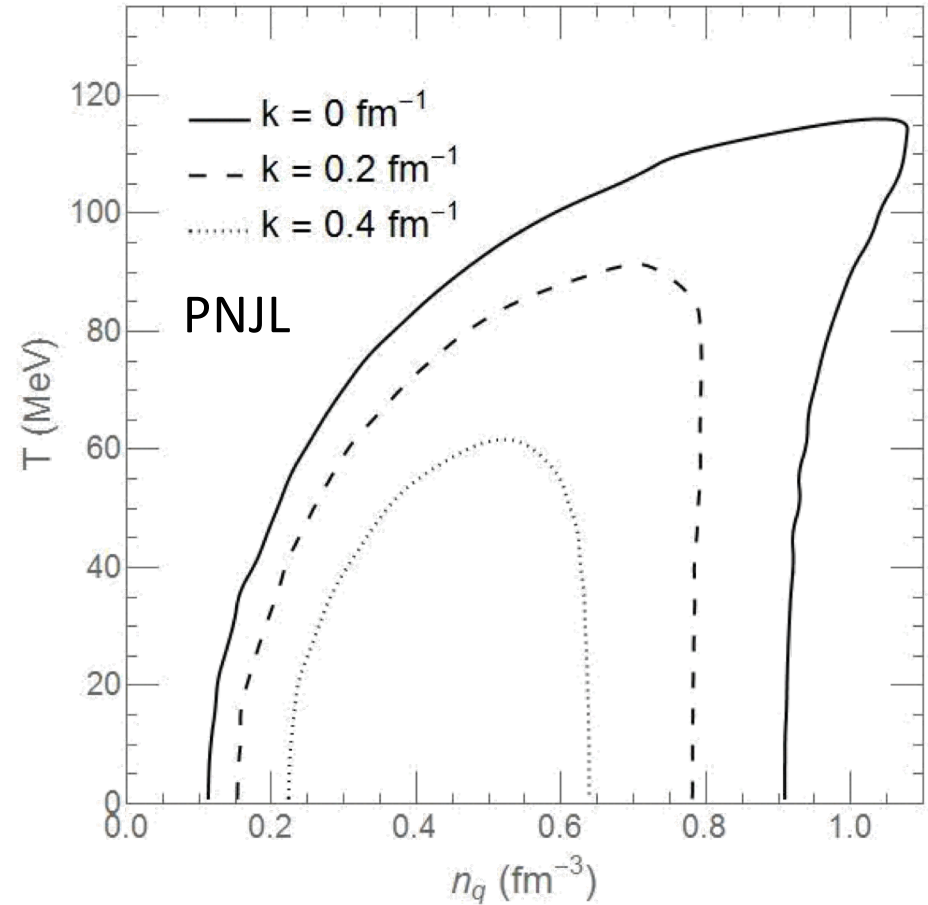
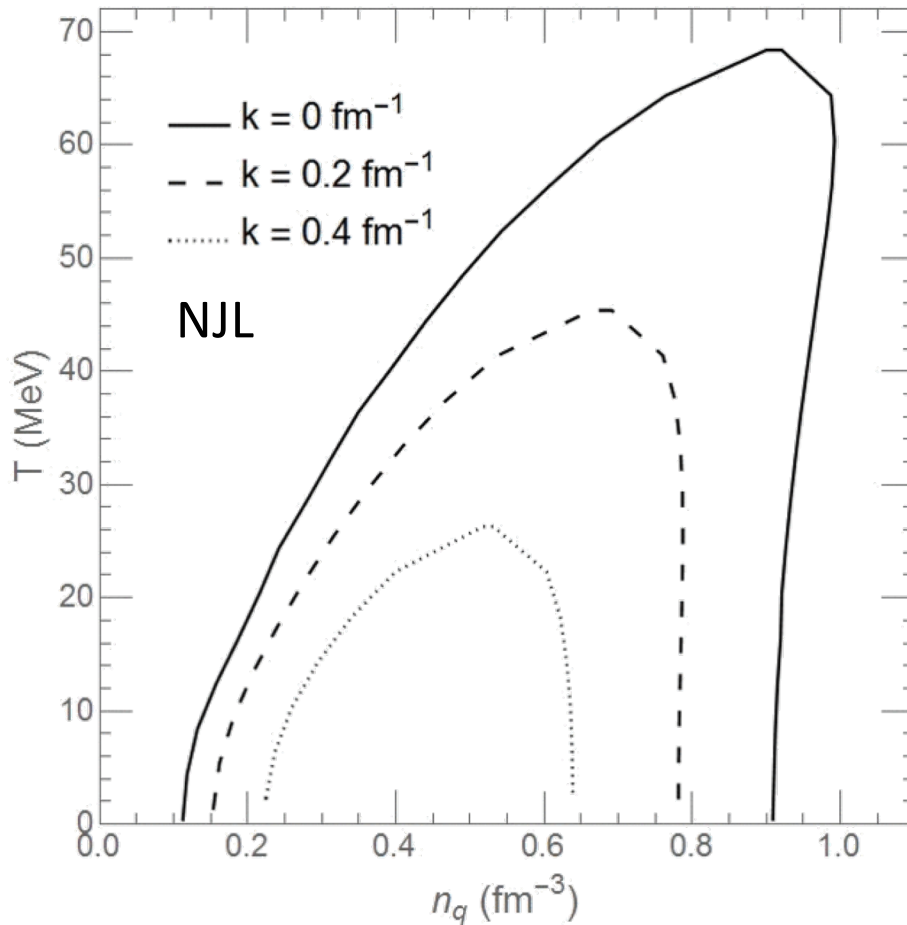
Fourier transform leads to

$$0 = (I - X(k)) \begin{pmatrix} \delta\tilde{\sigma}_q(k) \\ \delta\tilde{\sigma}_s(k) \\ \delta\tilde{j}^\mu(k) \end{pmatrix}$$

Nonzero solutions requires $\det |I - \chi(k)| = 0$

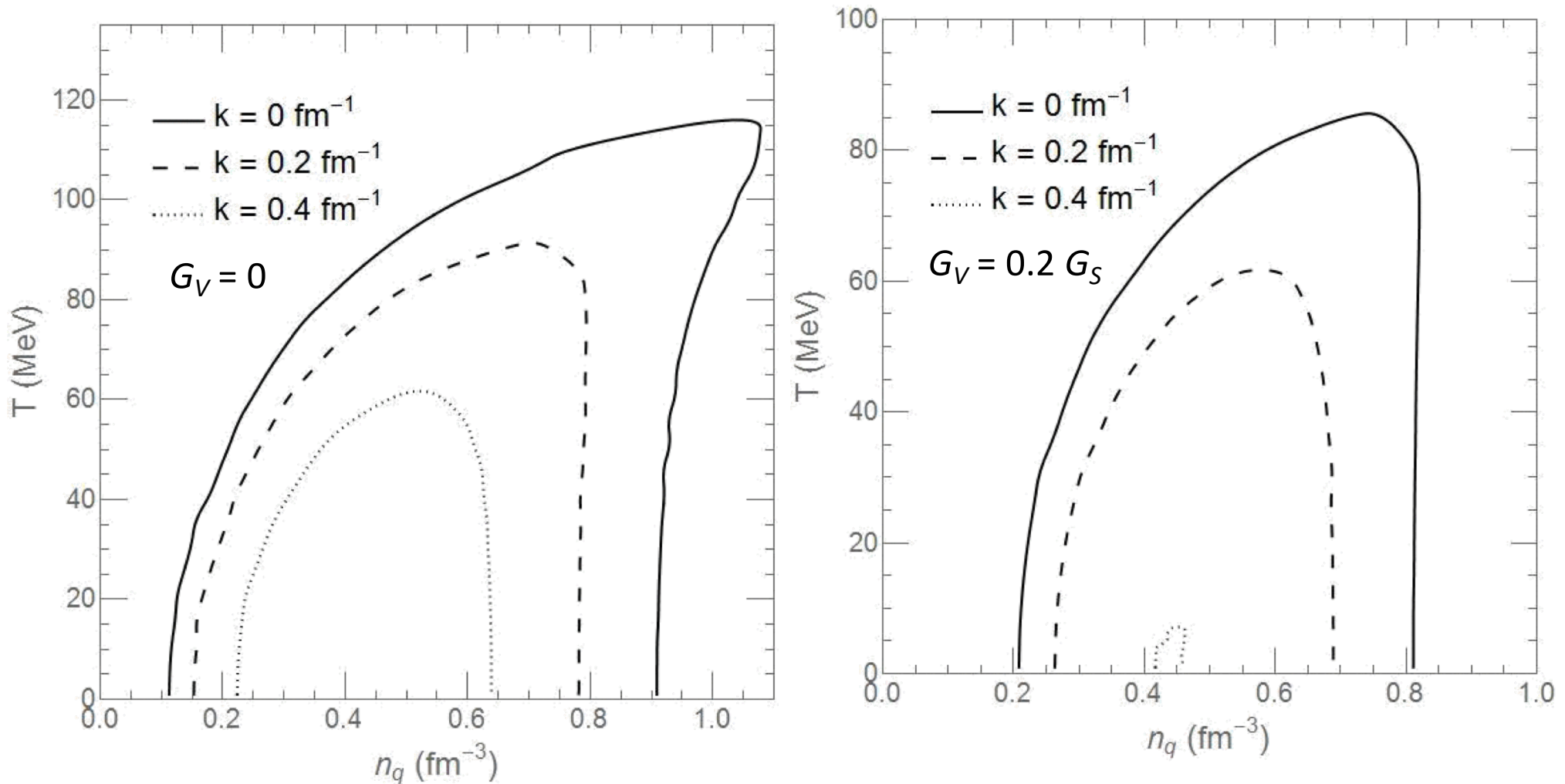
Solutions give the dispersion relation $k_0 = \omega_k$ of collective modes.

Spinodal boundaries of unstable modes with $G_V=0$



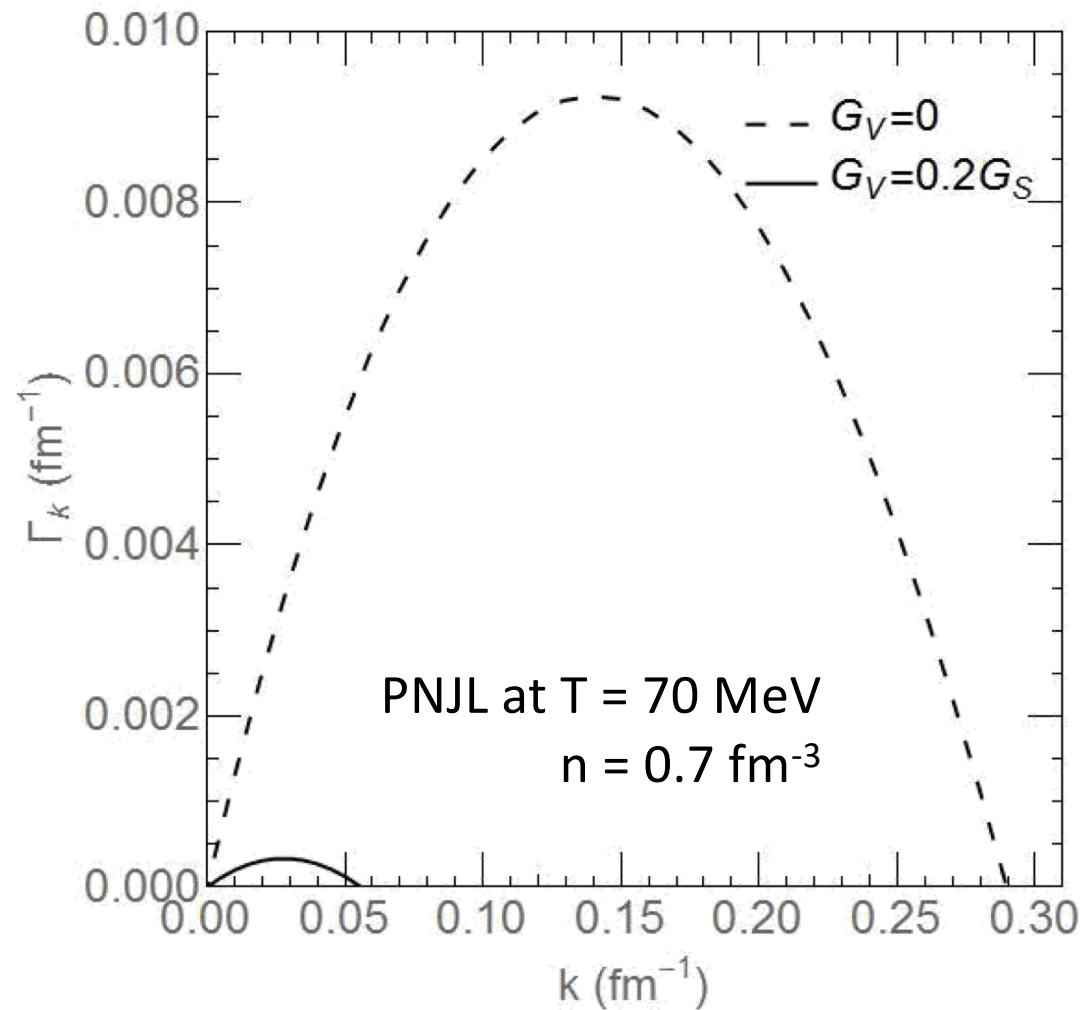
- Spinodal boundary shrinks with increasing wave number or decreasing wavelength and without Polyakov loop.

Spinodal boundaries of unstable modes with $G_V = 0.2 G_S$



- Spinodal boundary shrinks with increasing G_V .

Growth rate of unstable modes in quark matter



- Vector interaction reduces the growth rate of unstable modes.

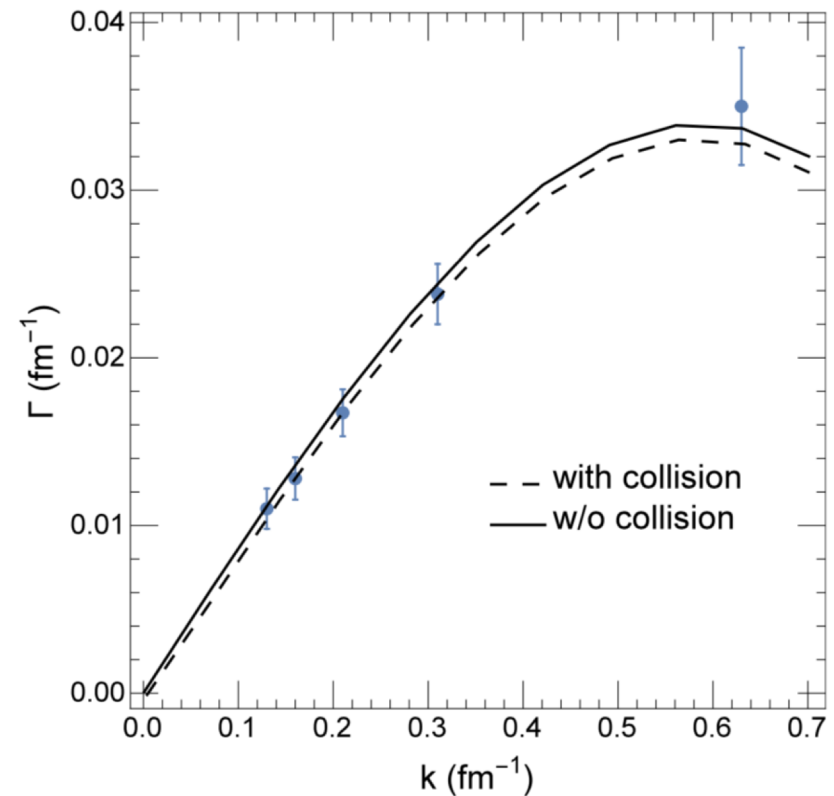
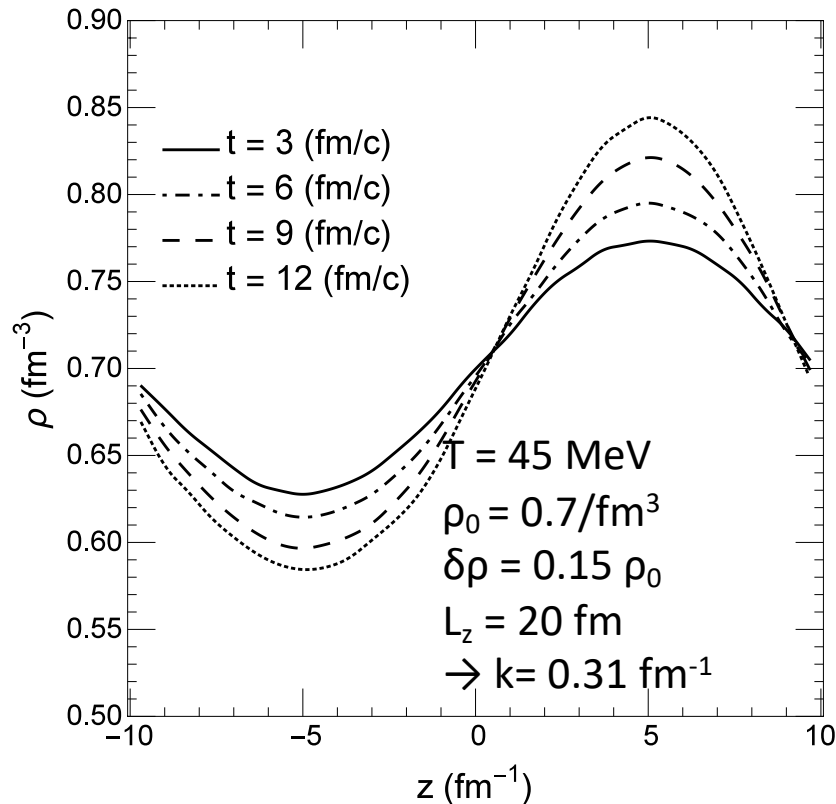
Vlasov description of quark matter in a box (NJL)

$$\partial_t f + \mathbf{p}/E \cdot \nabla f - \nabla H \cdot \nabla_p f = 0$$

Mean field $H = \sqrt{(M - 2G_S \langle \bar{q}q \rangle)^2 + (\mathbf{p} \mp 2G_V \langle \bar{q}\gamma\mathbf{q} \rangle)^2} \pm 2G_V \langle \bar{q}\gamma^0 q \rangle$

$$\rho(\mathbf{r}, t = 0) = \rho_0 + \delta\rho_0 \sin(2\pi z/L_z)$$

$$\delta\rho(t) = \delta\rho_0 \cosh(\Gamma_k t)$$

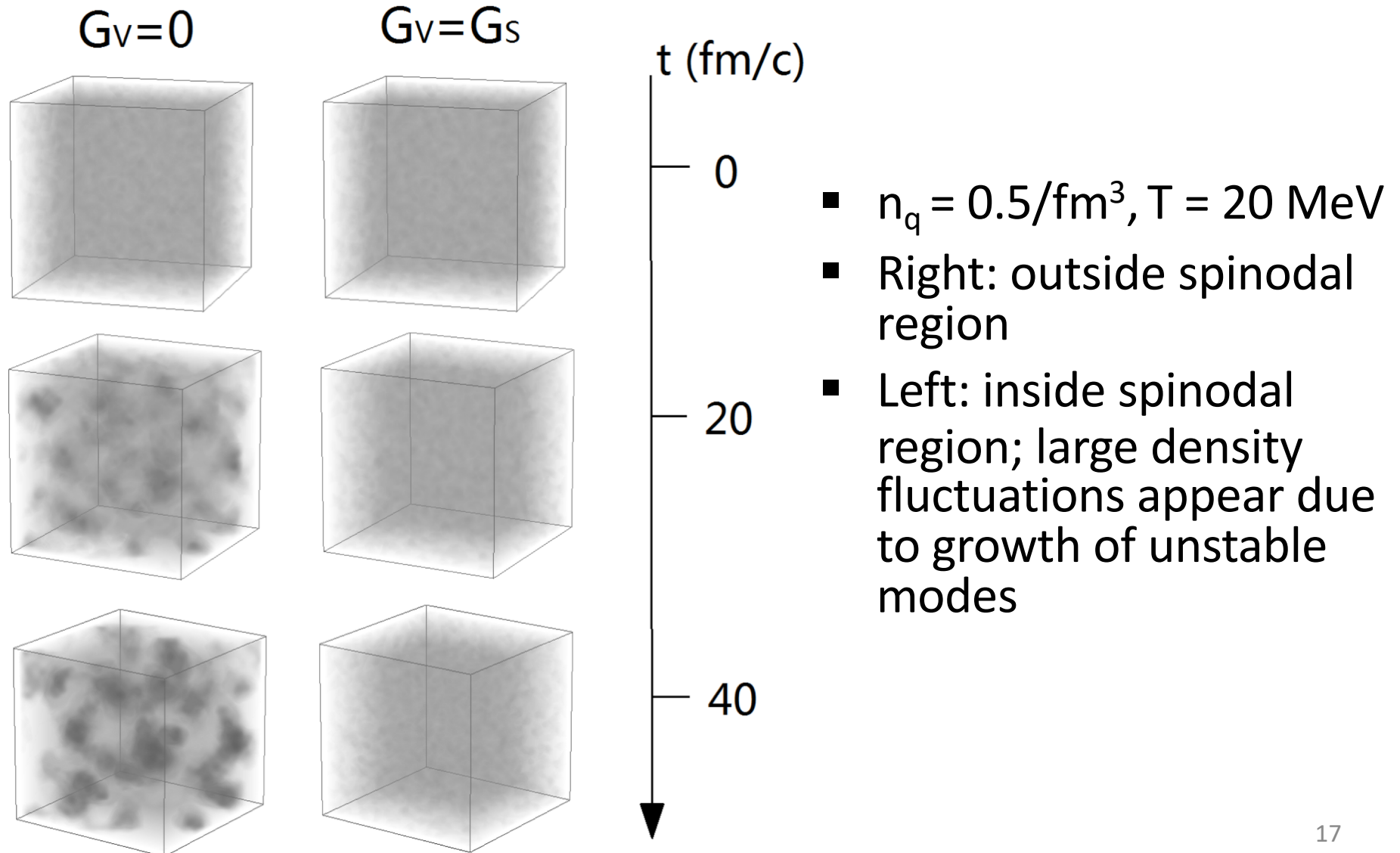


- Wave vector dependence of growth rate of unstable modes are consistent with that from linearized Boltzmann eq. and is not much affected by collisions.

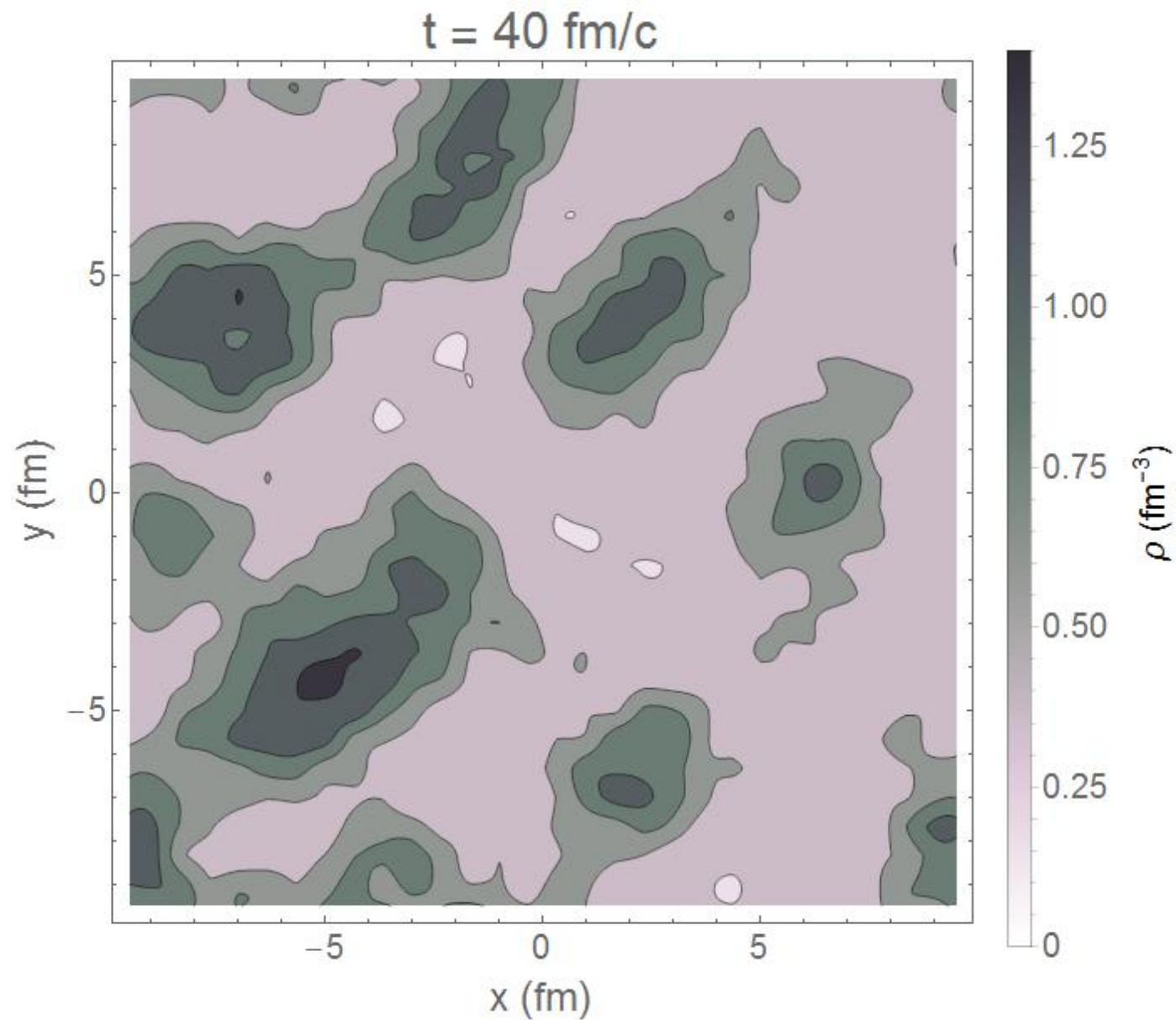
Transport description of quark matter in a box

$$\partial_t f + \mathbf{p}/E \cdot \nabla f - \nabla H \cdot \nabla_p f = \mathcal{C}[f]$$

$\mathcal{C}[f]$ includes quark elastic scattering with cross section of 3 mb

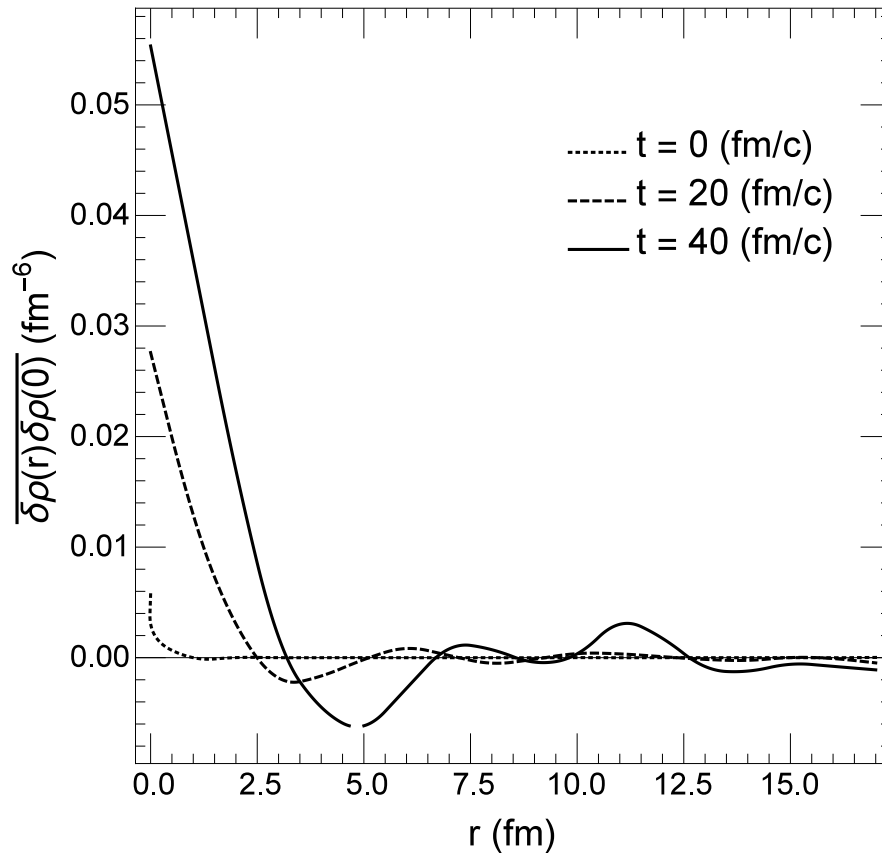


Cross sectional view of density fluctuation on $z = 0$ plane

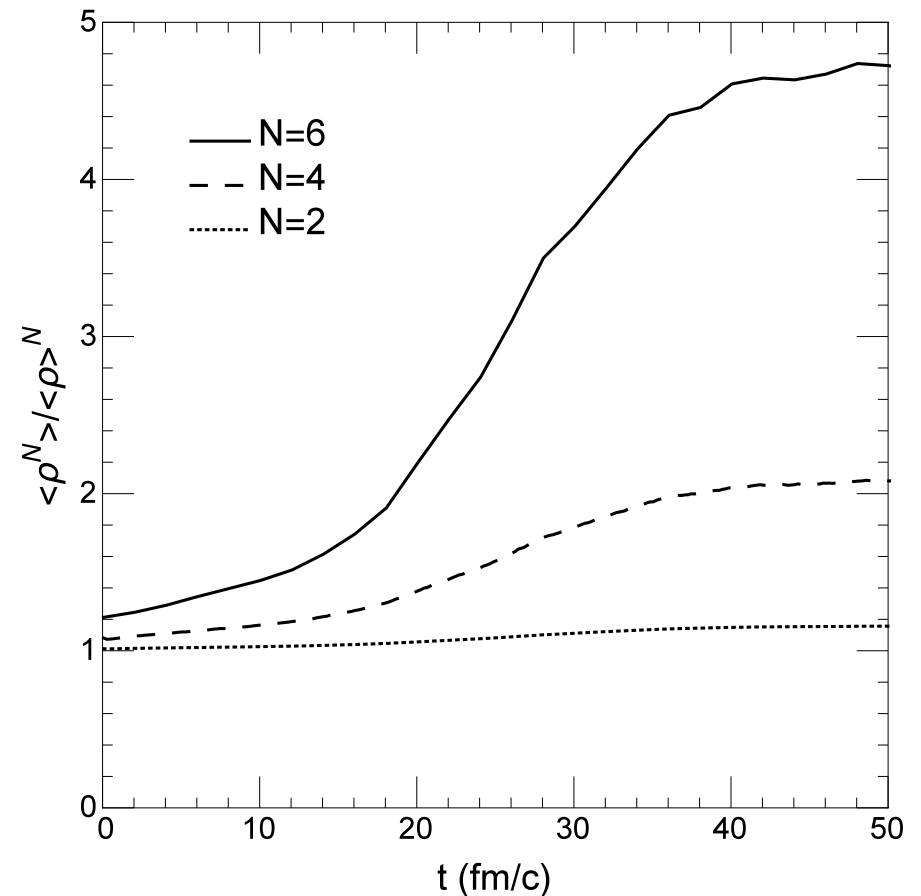


Characterization of density fluctuations

Density-density correlations

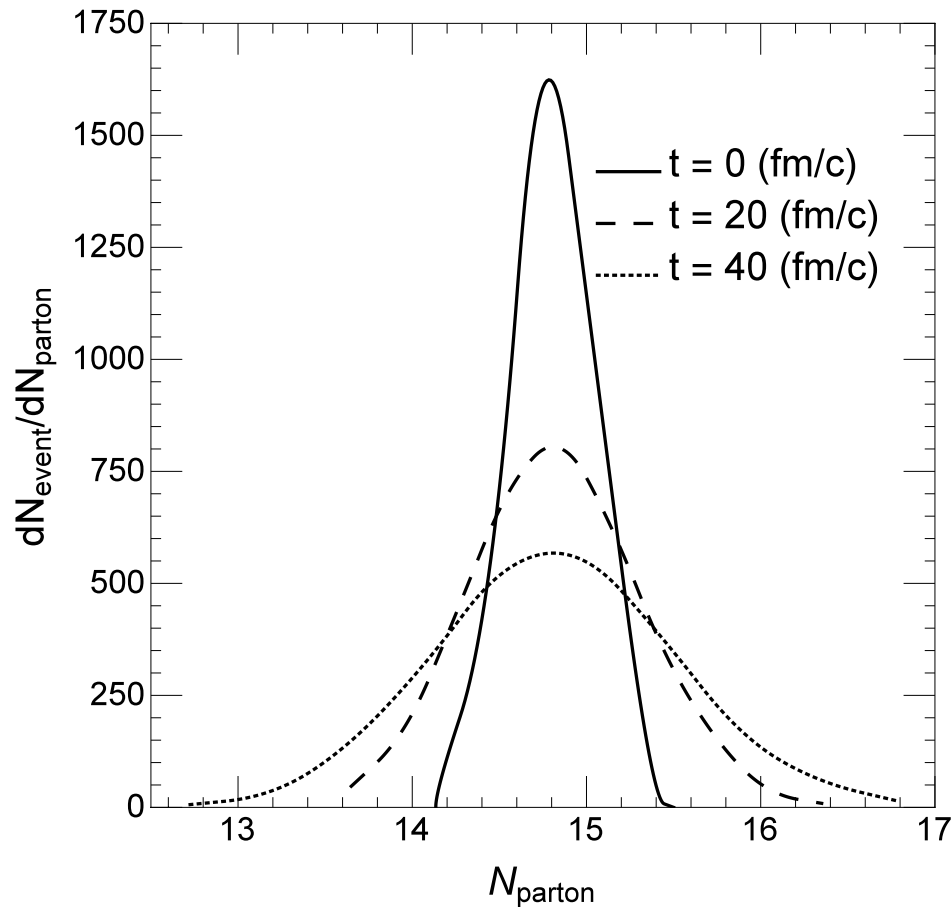


Moments $\langle \rho^N \rangle \equiv \frac{1}{A} \int d^3\mathbf{r} \rho^{N+1}(\mathbf{r})$

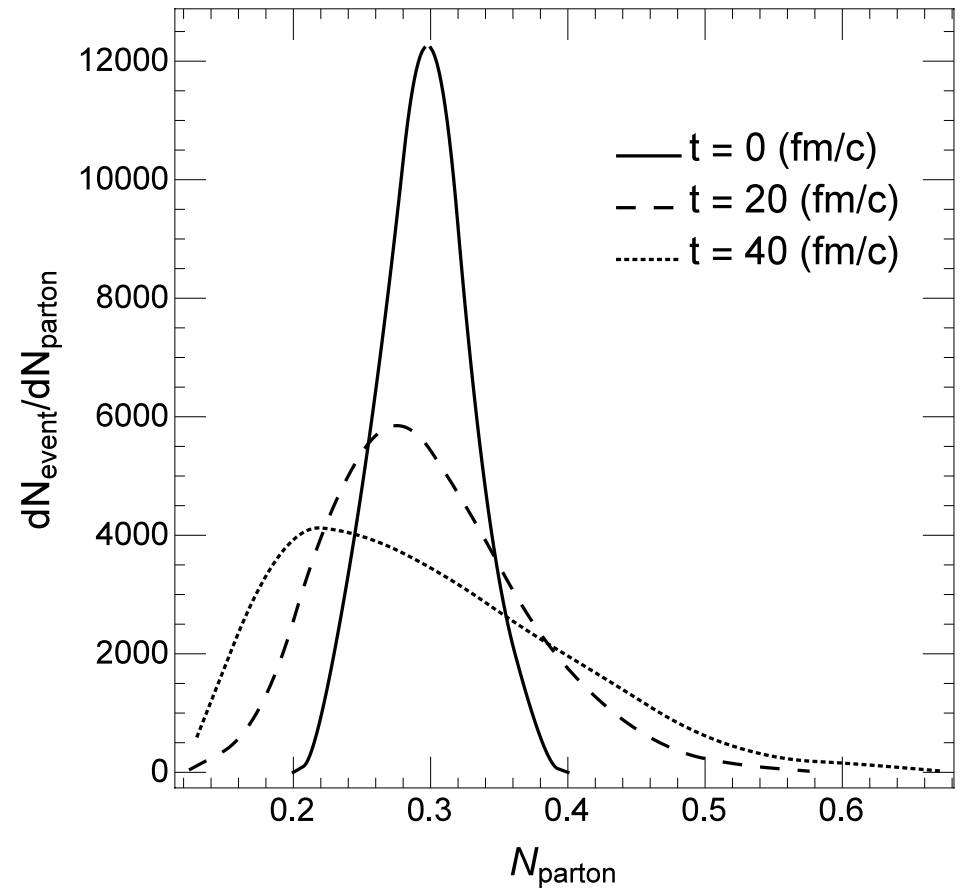


- Spinodal instability leads to longer range in density-density correlations and large density moments.

Event-by-event fluctuations of parton number in a sub-volume



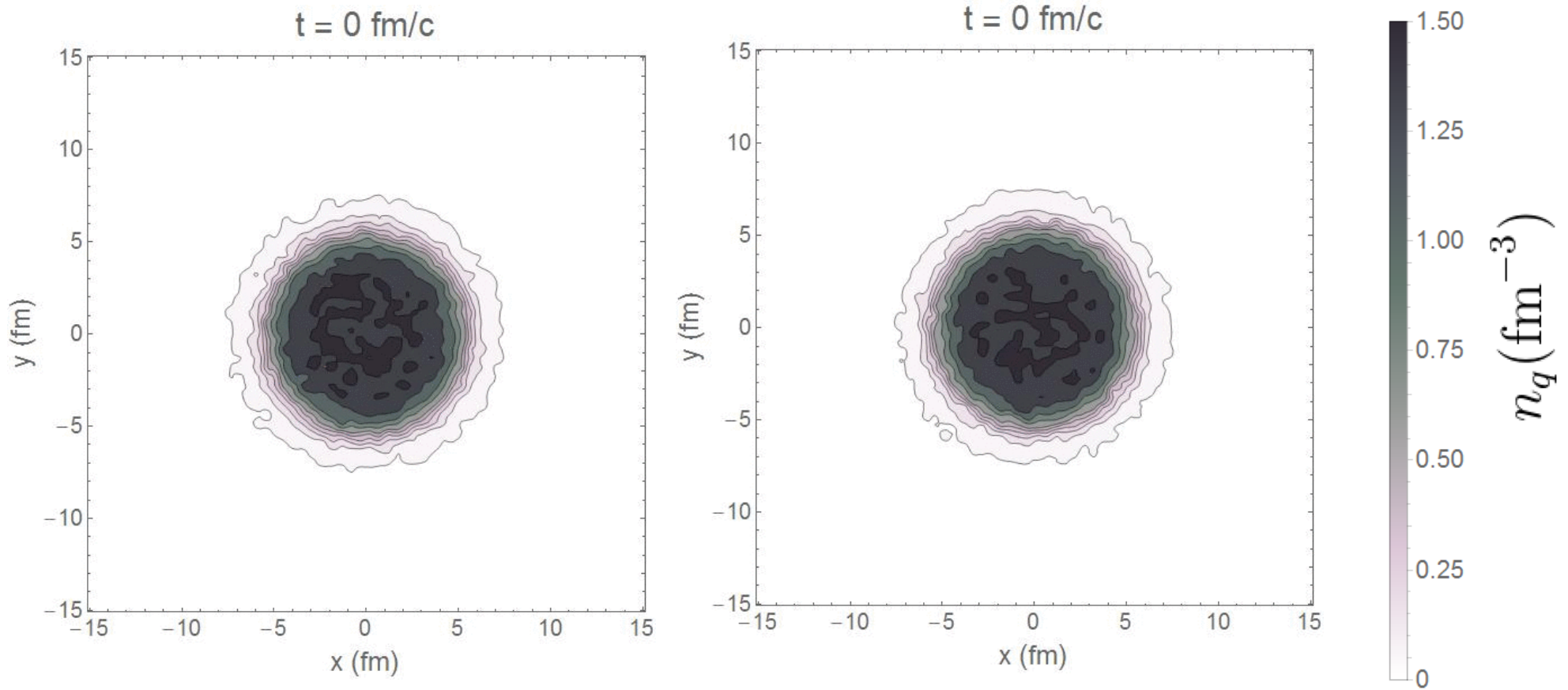
$$\Delta V = 30 \text{ fm}^3$$



$$\Delta V = 0.6 \text{ fm}^3$$

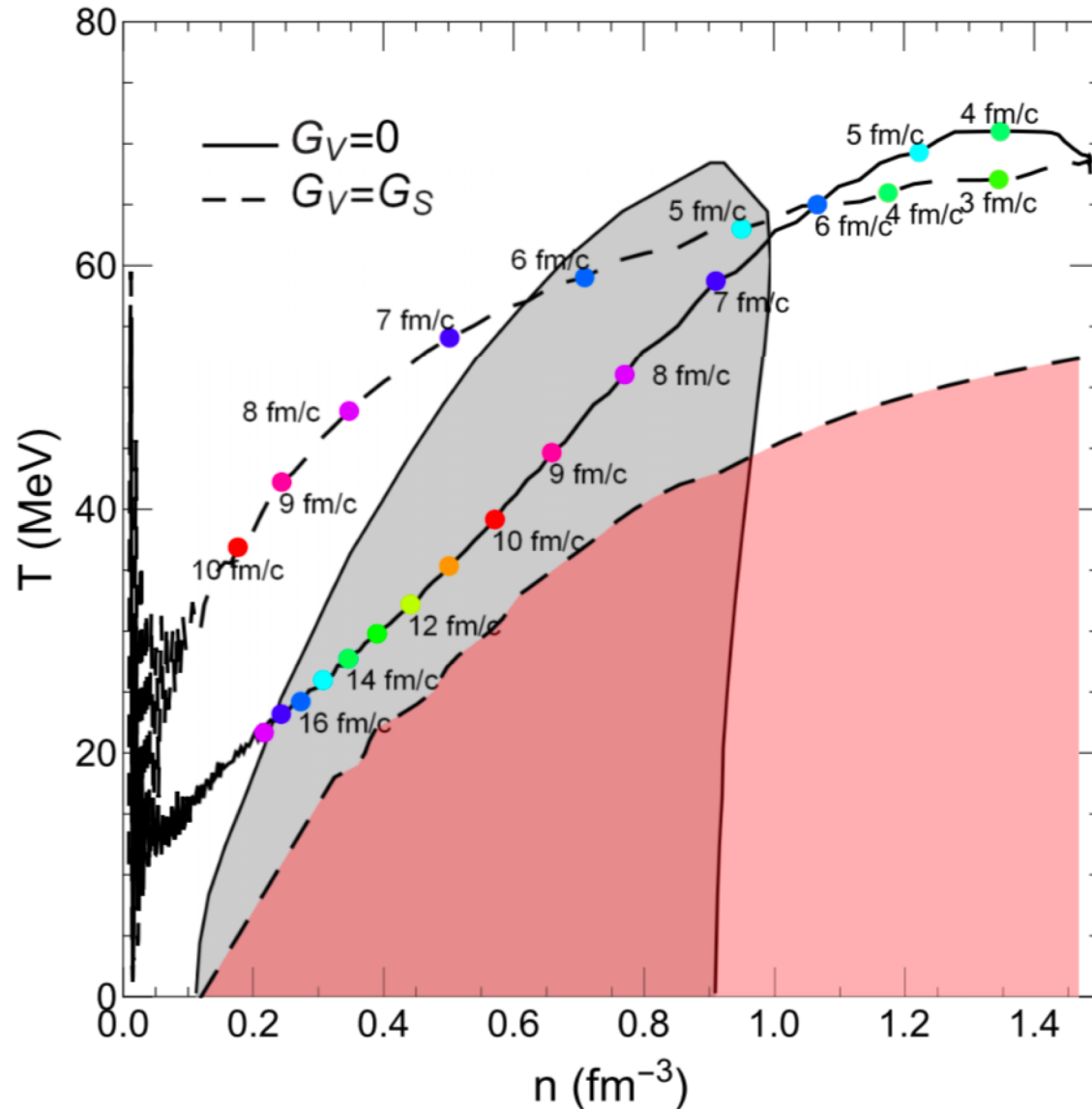
- Increasing skewness ($\langle \delta N^3 \rangle / \langle \delta N^2 \rangle^{3/2}$) with time in small sub-volume.

Expanding quark matter: blast-wave initial conditions



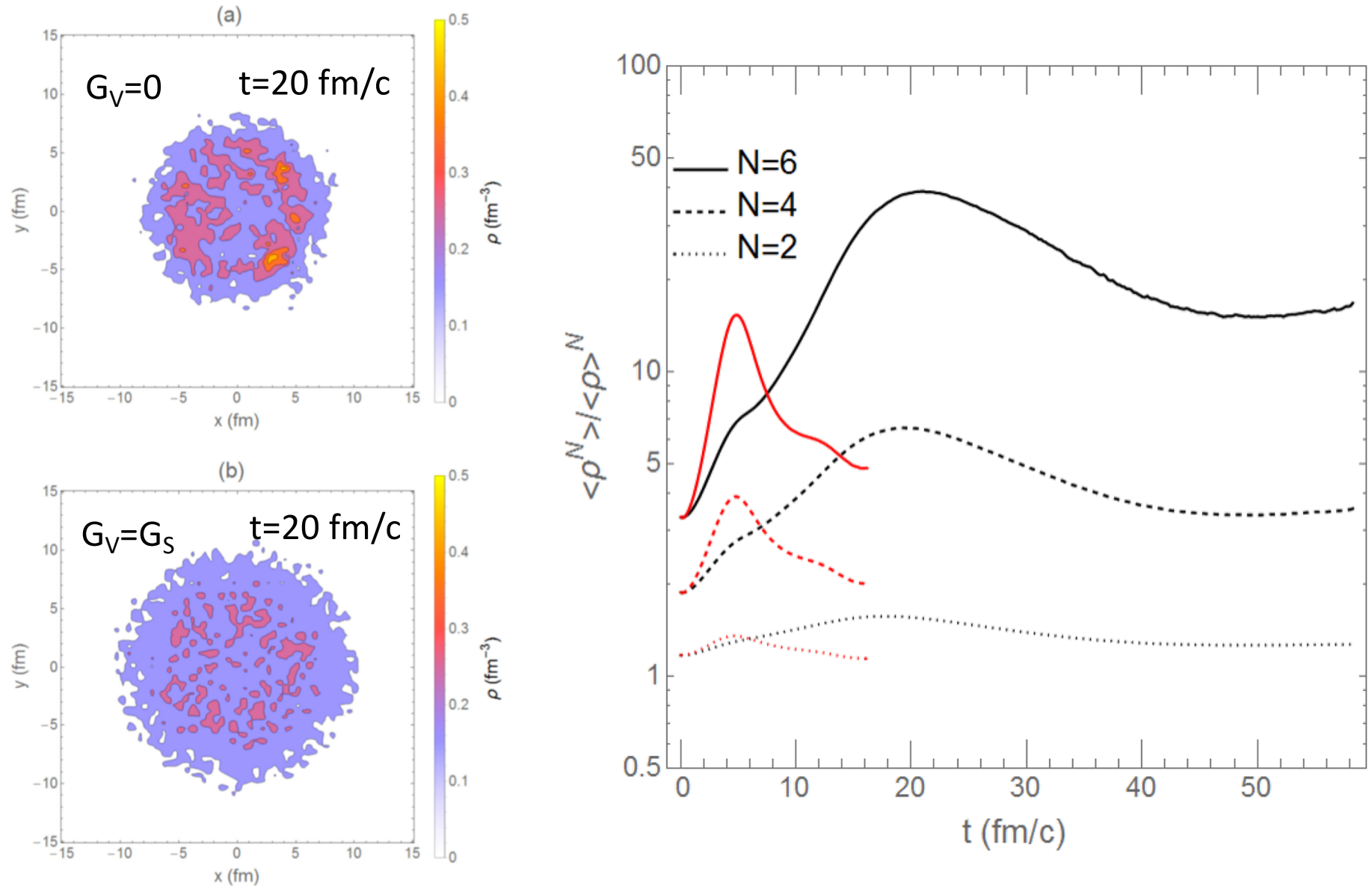
- Initial $n_q = 1.5/\text{fm}^3$, $T = 70 \text{ MeV}$
- Left: $G_V = 0$, with 1st-order transition
- Right: $G_V = G_S$, no 1st-order transition
- 1st-order transition leads to large density fluctuation

Trajectory of an expanding quark matter



- First-order phase transition results in a longer QGP phase of an expanding dense matter.

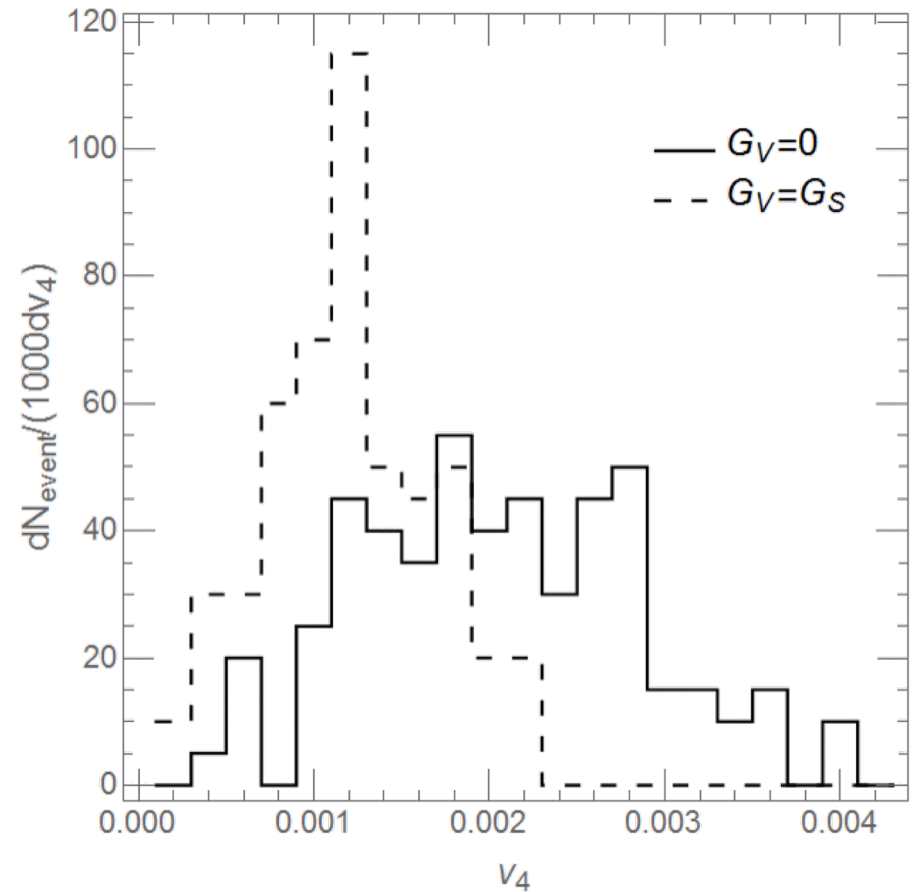
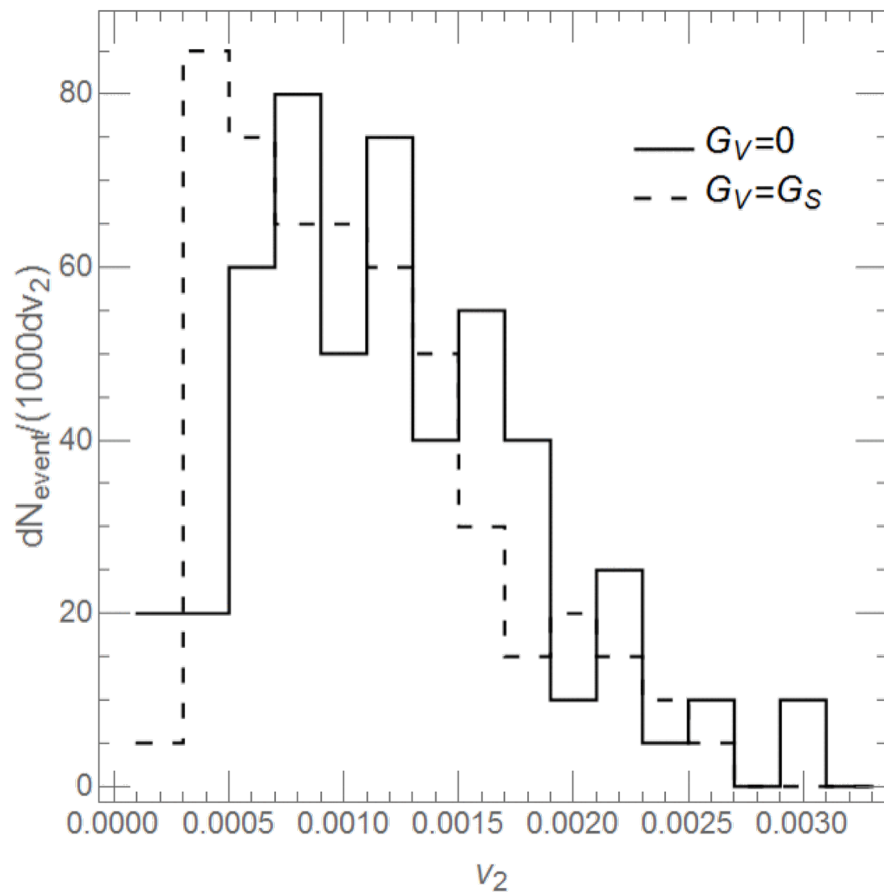
Time evolution of density moments



- Large density moments are generated by the spinodal instability.

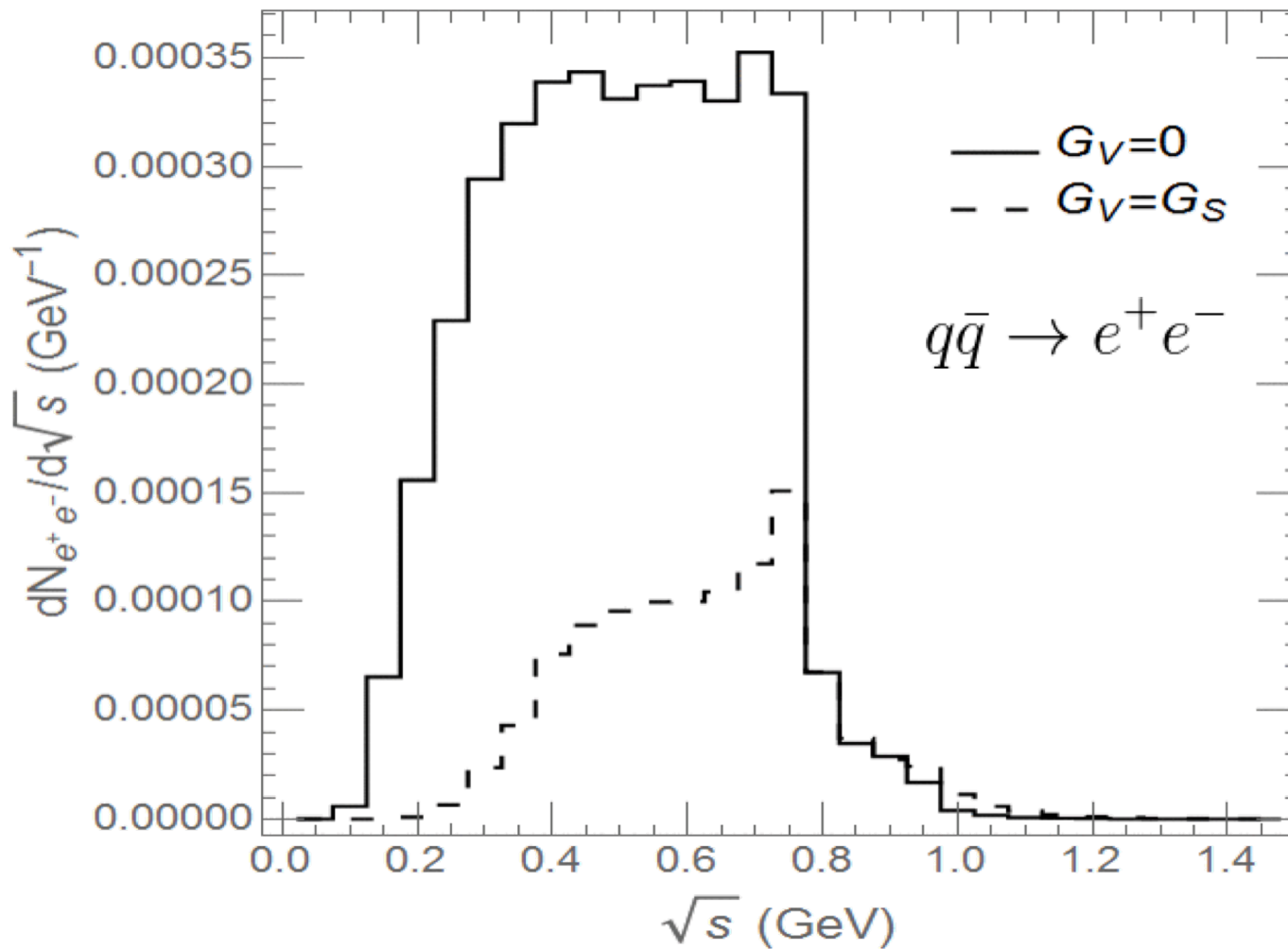
Anisotropic flows

$$f(p_T, \phi) = \frac{N(p_T)}{2\pi} \left\{ 1 + 2 \sum_{n=1}^{\infty} v_n(p_T) \cos[n(\phi - \psi_n)] \right\}$$



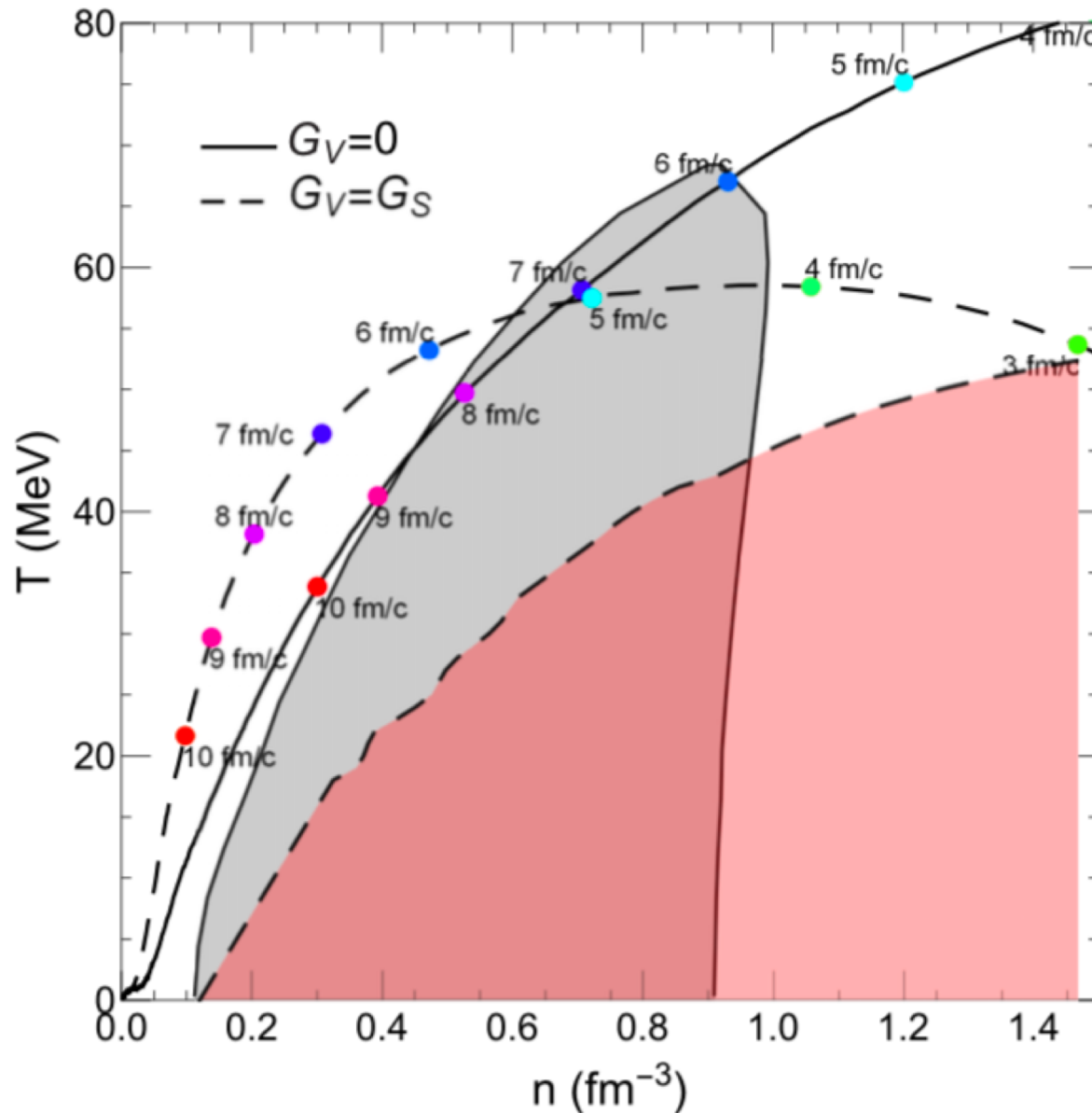
- Density fluctuations result in nonzero anisotropic flows.

Dilepton production

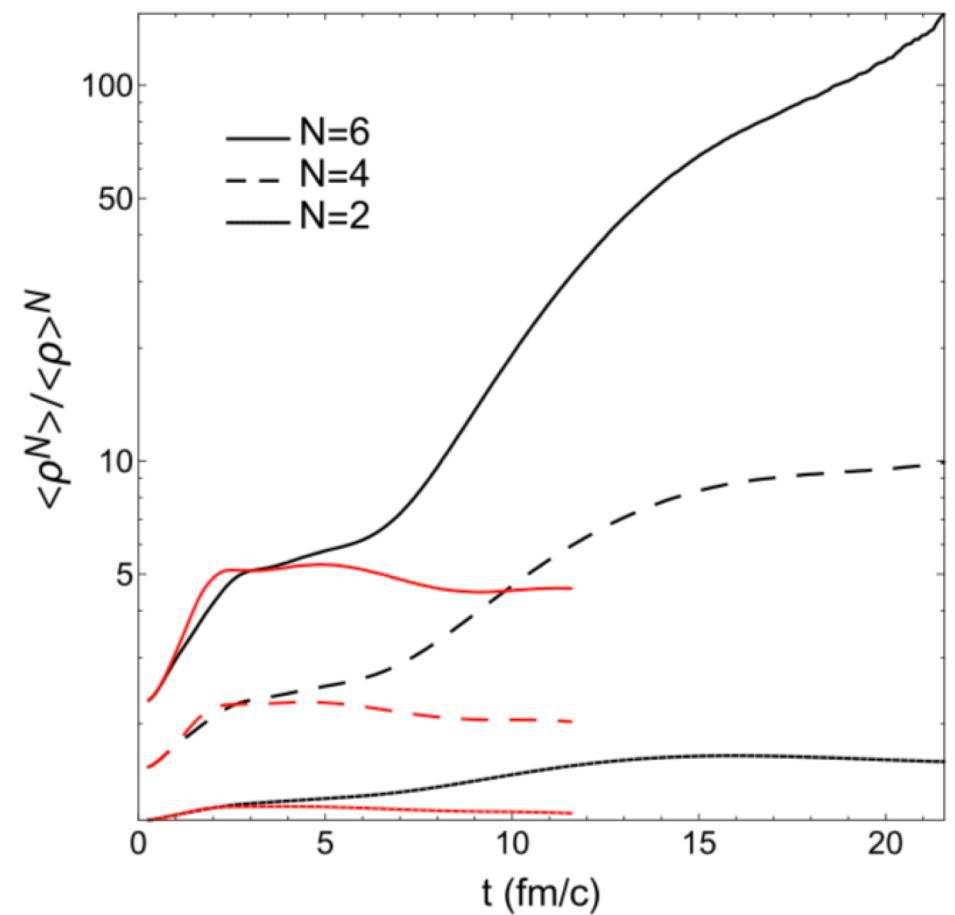
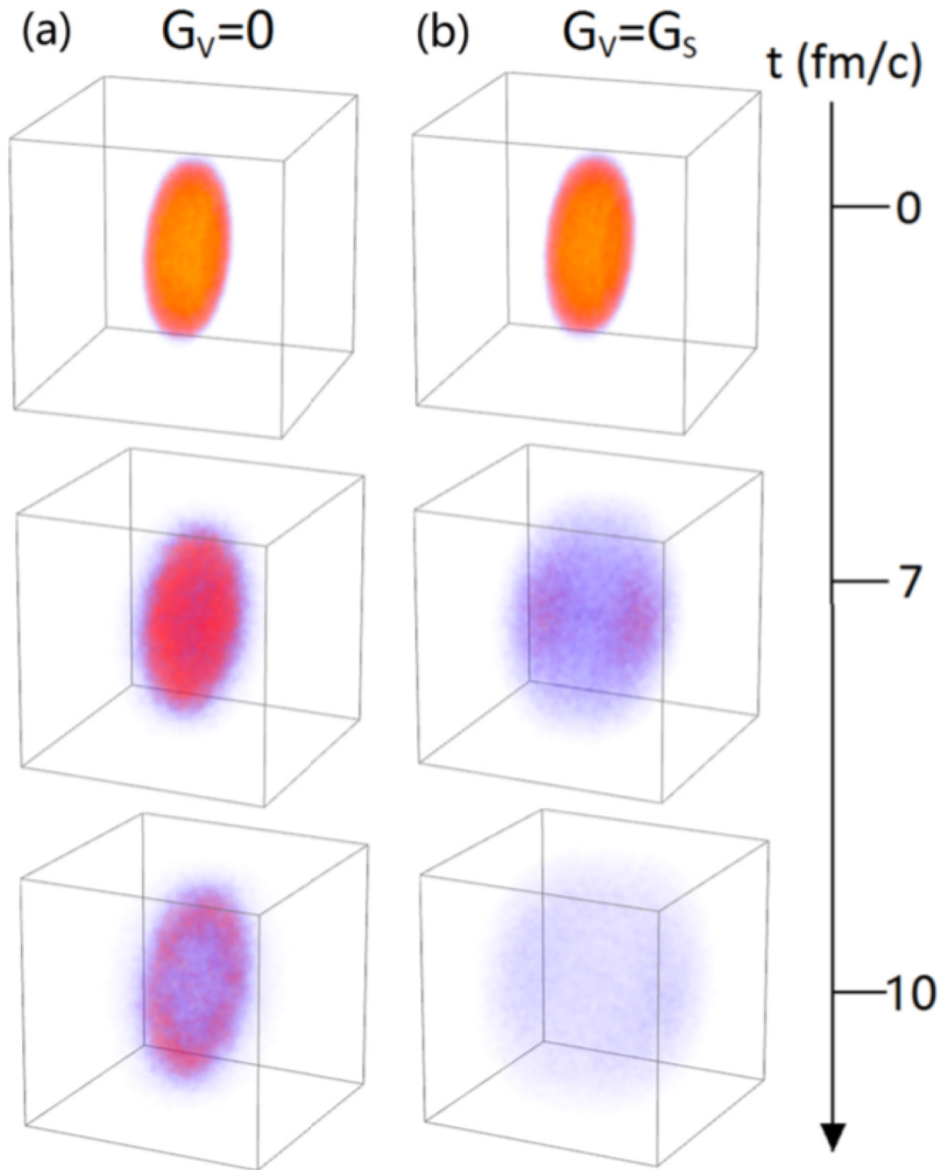


- Enhanced dilepton production due to density fluctuations

Expanding quark matter: AMPT initial conditions ($v_{s_{NN}} = 2.5$ GeV)

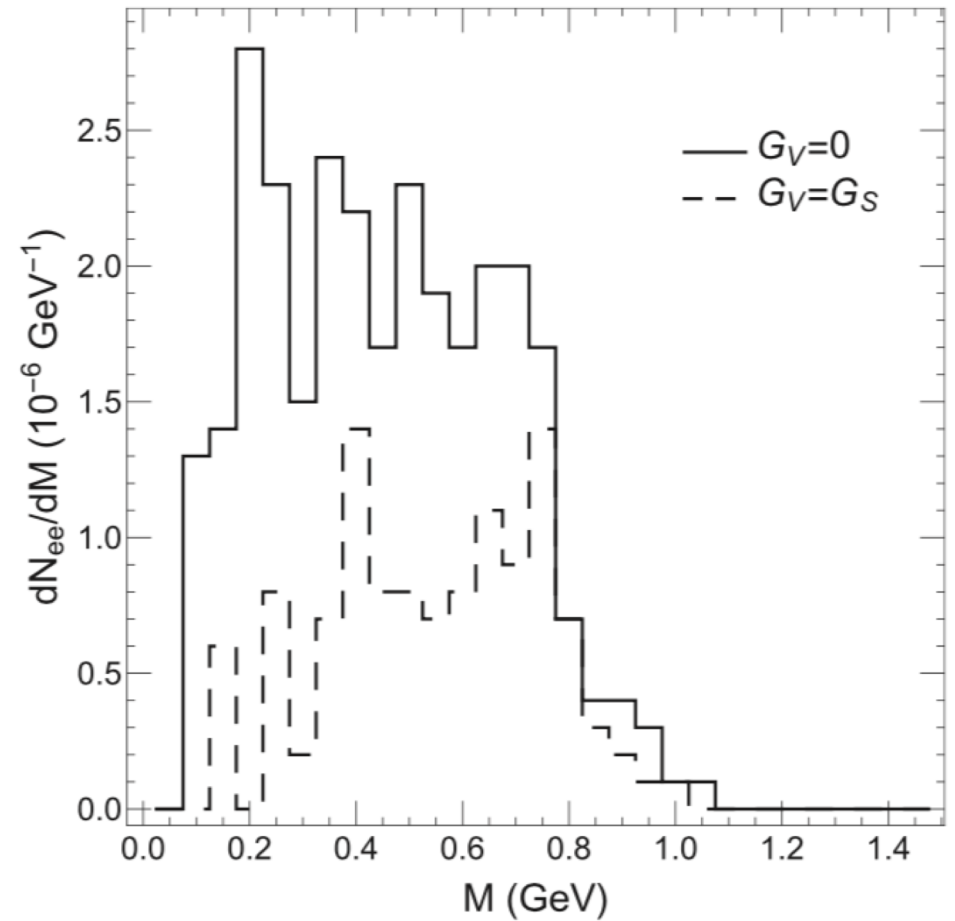
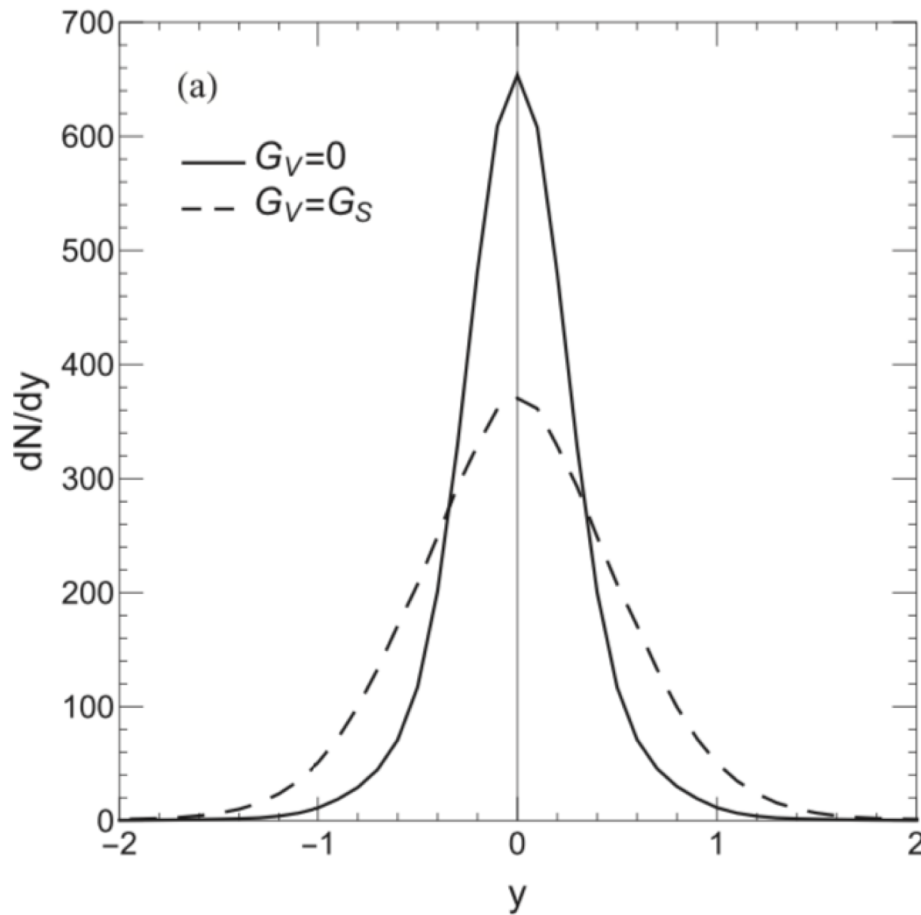


Time evolution of density moments



- Large density moments are generated by the spinodal instability.

Effects of density fluctuations



- Narrower rapidity distribution
- Enhanced dilepton production

Summary

- Critical temperature in the PNJL model is almost twice that in the NJL model.
- Both the vector interaction and the quantum (or finite range) effect suppress the spinodal instability. The former suppression is seen for all unstable modes, while the latter suppression acts only on unstable modes of short wavelength.
- High-order density moments increase and saturate at large values after phase separation.
- Expansions are slowed by the presence of a first-order phase transition.
- Anisotropic flow, dilepton yield, and rapidity distribution are possible signals of a first order-phase transition from the quark to the hadronic matter.
- Survival of density fluctuation after hadronic evolution may be responsible for the enhanced production of light nuclei in HIC.